Ventricular Function and Dyssynchrony Quantified by Speckle-Tracking Echocardiography in Patients with Acute and Chronic Right Ventricular Pressure Overload

Kazuhide Ichikawa, MD, Kaoru Dohi, MD, PhD, Emiyo Sugiura, MD, PhD, Tadafumi Sugimoto, MD, PhD, Takeshi Takamura, MD, PhD, Yoshito Ogihara, MD, Hiroshi Nakajima, MD, PhD, Katsuya Onishi, MD, PhD, Norikazu Yamada, MD, PhD, Mashio Nakamura, MD, PhD, Tsutomu Nobori, MD, PhD, and Masaaki Ito, MD, PhD, *Tsu and Ise, Japan*

Background: The aim of this study was to noninvasively investigate right ventricular and left ventricular (LV) adaptation to right ventricular pressure overload in patients with acute pulmonary thromboembolism (APTE) and chronic pulmonary artery hypertension (CPAH).

Methods: Thirty-seven patients with APTE, 36 patients with CPAH, and 33 controls were retrospectively enrolled. Myocardial deformation and wall motion were analyzed using speckle-tracking strain and displacement imaging echocardiography in the right and left ventricles. The standard deviation of the heart rate–corrected intervals from QRS onset to peak systolic strain and peak systolic displacement (PSD) for the six segments was used to quantify right ventricular and LV mechanical dyssynchrony (peak systolic strain dyssynchrony and PSD dyssynchrony). The myocardial performance index in both ventricles was also evaluated.

Results: The APTE and CPAH groups had reduced ventricular performance (LV myocardial performance index, 0.40 ± 0.10, 0.66 ± 0.18 [*P* < .05 vs controls], and 0.58 ± 0.19 [*P* < .05 vs controls] in the control, APTE, and CPAH groups, respectively) and large mechanical dyssynchrony (LV longitudinal PSD dyssynchrony, 58 ± 41 msec, 119 ± 49 msec [*P* < .05 vs controls], and 83 ± 37 msec [*P* < .05 vs controls and the APTE group] in the control, APTE, and CPAH groups, respectively) in both ventricles. Multiple regression analysis indicated that LV longitudinal PSD dyssynchrony in the APTE group and the LV eccentricity index in the CPAH group were independent determinants of LV myocardial performance index.

Conclusions: Pathophysiologic mechanisms that regulate ventricular performance vary depending on whether the ventricles are exposed to acute or chronic right ventricular pressure overload. (J Am Soc Echocardiogr 2013;26:483-92.)

Keywords: Echocardiography, Dyssynchrony, Ventricular interdependence, Acute pulmonary thromboembolism, Chronic pulmonary artery hypertension

Right ventricular (RV) pressure overload affects left ventricular (LV) performance via ventricular interdependence. Because of ventricular interdependence within the restricted intrapericardial space, marked RV dilatation causes a significant alteration in LV geometry and exerts a constraining effect on LV performance.[1,2] Recent clinical studies have demonstrated that RV pressure overload induces RV mechanical dyssynchrony.[3,4] In addition, impairment of LV mechanical synchrony can also be observed in the setting of RV pressure overload and has the potential to contribute to further deterioration of LV performance. We previously and independently reported that acute and chronic RV pressure overload negatively affected LV mechanical synchrony associated with LV functional impairment.[5,6] However, it has not been determined if the contribution of RV and LV mechanical dyssynchrony to each ventricle's performance varies depending on whether the heart is exposed to acute or chronic RV pressure overload. Speckle-tracking strain and displacement echocardiography can measure global and regional myocardial kinetics, including mechanical dyssynchrony, independent of echo angle and chamber translation.[7] Accordingly, we extended our previous investigation[5,6] and investigated the potential role of regional wall motion abnormalities and mechanical dyssynchrony in the pathophysiologic processes leading to development of LV functional deterioration using speckle-tracking echocardiography in combination with quantitative assessment of ventricular geometric remodeling in patients with acute pulmonary

thromboembolism (APTE) and chronic pulmonary artery hypertension (CPAH).

METHODS

Study Population

A total of 86 consecutive patients with massive or submassive APTE ($n = 40$) and CPAH ($n = 46$) who were referred to Mie University Hospital between May 2005 and March 2012 were retrospectively screened for inclusion in this study. The diagnosis of APTE was confirmed or excluded using a combination of personal history, physical examination, laboratory tests, electrocardiography, echocardiography, thoracic computed tomography, and right heart catheterization, as previously described.[3,5,6,8-10] All patients with CPAH met the restrictive criteria of a diagnosis of pulmonary artery hypertension by right heart catheterization, and their etiology had been identified by personal history, physical examination, laboratory tests, echocardiography, and thoracic computed tomography. We excluded three patients with APTE because of suboptimal images. We also excluded 10 patients with CPAH (four with atrial fibrillation, four with ischemic heart disease, one with a pacer wire in the right ventricle, and one with technically inadequate images). Accordingly, the patient study groups consisted of 37 subjects with APTE (mean age, 61 ± 15 years) and 36 with CPAH (mean age, 55 ± 19 years). Twenty-five of 37 patients with APTE and 17 of 36 patients with CPAH in this study had been included in previously published reports.[3,5,6] We also studied 33 age-matched normal subjects (the control group; mean age, 57 ± 14 years) who had no histories of cardiopulmonary disease, normal electrocardiographic results, and normal echocardiographic results. Twenty-five of the 33 control subjects in this study had also been included in previously published reports.[3,5,6] The protocol was approved for use by the Human Studies Subcommittee of Mie University Graduate School of Medicine.

Echocardiography

All subjects underwent complete transthoracic echocardiography using a Vivid 7 system (GE-Vingmed Ultrasound AS, Horten, Norway), as previously described.[3,5,6] Echocardiography was performed on hospital admission (4 ± 5 days after initial symptoms) but before initiating primary treatment in all patients with APTE. The mean duration of symptomatic pulmonary hypertension was 52 ± 69 months until echocardiographic examination in patients with CPAH. Arm-cuff blood pressure measurements were performed at the beginning of the echocardiographic study for all subjects. Peak systolic pulmonary artery pressure was calculated from the sum of the mean right atrial pressure, as estimated by the diameter of the inferior vena cava and its respiratory variation,[11] and the maximal pressure difference between the right ventricle and the right atrium, as calculated by the continuous-wave Doppler flow velocity.[5] The RV end-diastolic area index, the end-systolic area index, and the fractional area change from the apical four-chamber view were also measured.[5] Pulmonary vascular resistance (PVR) was noninvasively estimated us-

ing echocardiography.[12] LV volume indices and ejection fraction were assessed using the biplane Simpson's rule. The LV eccentricity index, defined as the ratio of the LV anterior-to-posterior dimension to the septal-to-lateral dimension at end-diastole from the midventricular short axis image, was used as an index of septal geometric abnormality caused by RV diastolic pressure overload.[6,13] The Doppler-derived stroke volume was normalized to body surface area. The ratio of peak early to late diastolic transmitral flow velocity (mitral E/A) was calculated using pulsed Doppler echocardiography.[14] Peak early diastole mitral annular velocity (Ea) at the inferior septum was measured from the apical four-chamber view. The E/Ea ratio was calculated as a Doppler parameter reflecting LV diastolic pressure.[15] The myocardial performance indexes (MPIs) in the left and right ventricles was assessed as previously described.[16,17] Systemic vascular resistance was calculated as follows: systemic vascular resistance (Wood units) = (mean arterial blood pressure − mean right atrial pressure)/ cardiac output. All echocardiographic measurements represent the average of three beats.

Speckle-Tracking Strain and Displacement Analysis

Speckle-tracking analysis was used to generate regional myocardial strain and displacement in both the left and right ventricles (Figures 1–3). RV and LV longitudinal strain and displacement were assessed in the apical four-chamber views. LV radial and circumferential regional strain and LV radial displacement were assessed in the parasternal short-axis views at the mid-LV level. We did not perform circumferential displacement analysis in the present study, because EchoPAC software (GE-Vingmed Ultrasound AS) has no capability to measure circumferential displacement. The average frame rate for the analysis was 76 ± 15 Hz. For speckle-tracking echocardiographic assessment, routine B-mode grayscale images were analyzed using EchoPAC. Myocardial strain is expressed as the percentage change from the original dimension at end-diastole, myocardial thickening or lengthening was represented as a positive value, and myocardial thinning or shortening was represented as a negative value.[7,14] Myocardial displacement toward the contractile center in the short-axis view or toward the apex in the longitudinal direction was represented as a positive value. The software automatically divided the short-axis and apical 4-chamber image into six standard segments (Figure 1). Peak systolic strain (PSS) and peak systolic displacement (PSD) obtained from time-strain and time-displacement curves were defined as the indices of myocardial systolic deformation and wall motion. The standard deviation of the heart rate–corrected regional time to PSD and time to PSS from the onset of QRS was used to quantify LV mechanical dyssynchrony (PSS dyssynchrony and PSD dyssynchrony, respectively). If there were multiple distinct peaks, the largest peak was taken as the PSS or PSD. Although PSS or PSD occurs at or near aortic valve closure, the timing of these events may be shortened or prolonged, occurring well after aortic valve closure in various cardiac diseases. Accordingly, time to PSS and time to PSD were measured throughout the whole cardiac cycle.

Statistical Analysis

Data are presented as mean ± SD. The association among indices of cardiac function was investigated using regression analysis. Between-group comparisons were assessed using analysis of variance for continuous variables and Fisher's exact tests for categorical data. Bonferroni's correction was applied for multiple comparisons. Intraobserver variability was determined by having one observer
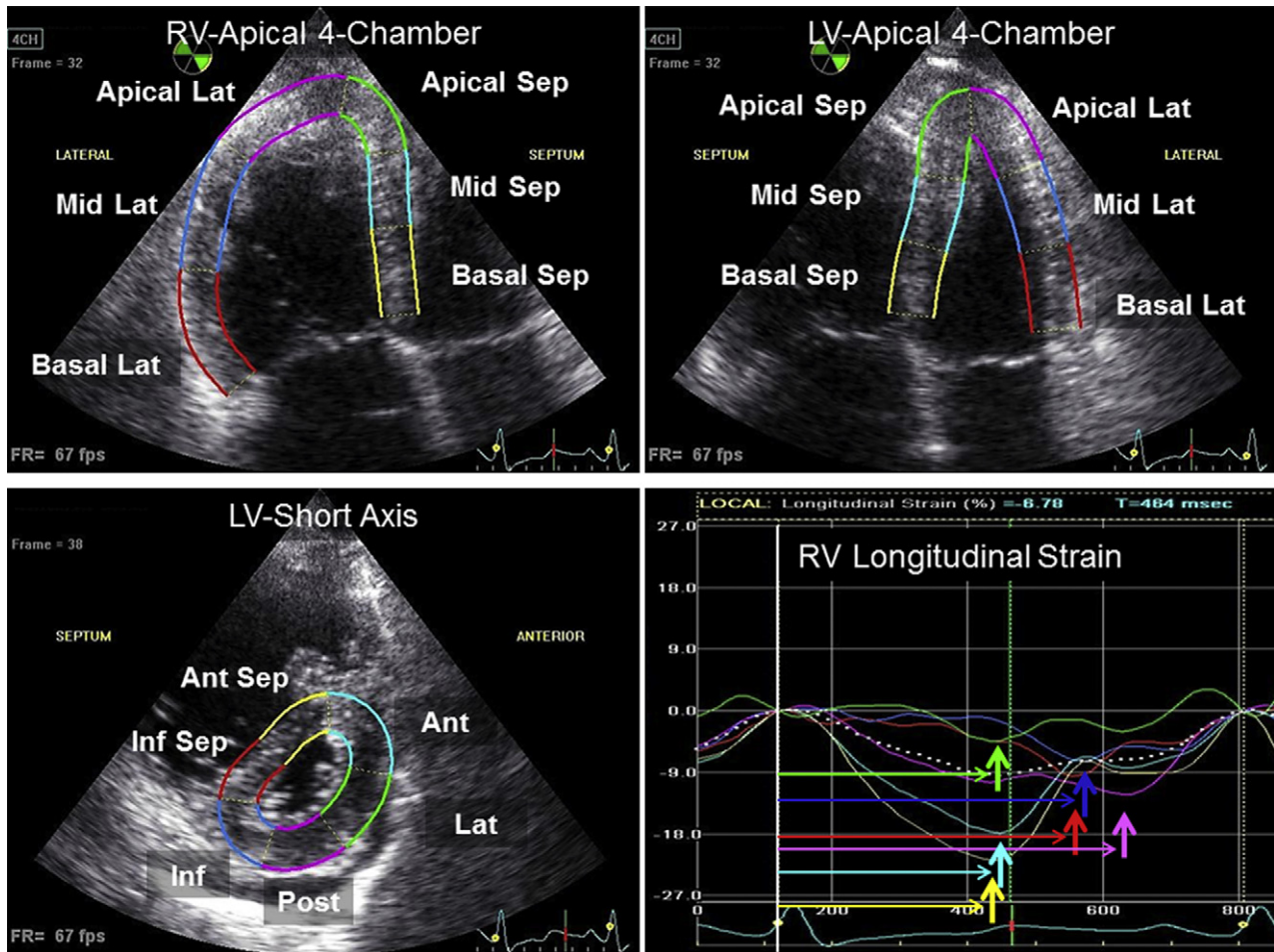
Figure 1 Six-segment models were created using a tracking algorithm after manual delineation of the endocardial border in the long axis views in the *right* ventricle (*left top*) and in the *left* ventricle (*right top*) from the apical approach and the short-axis view for the LV circumferential and radial functional measurements (*left bottom*). Example of time-strain curves in the RV longitudinal direction from a patient with acute massive pulmonary thromboembolism (*right bottom*). Solid *colored lines* represent segmental strain, and the *dotted white line* indicates global myocardial strain. *Colored vertical arrows* indicate segmental PSS, and corresponding *right arrows* indicate time to PSS.

repeat the measurements of time to PSS and time to PSD for each of the six segments in the RV longitudinal direction and the LV longitudinal, radial, and circumferential directions in 10 randomly selected subjects. Interobserver variability was determined by having a second observer measure these variables in the same data sets. Intraobserver and interobserver variability values were calculated as the absolute differences between the corresponding two measurements as a percentage of the mean. *P* values < .05 were considered statistically significant. Analyses were performed using SPSS for Windows version 19 (SPSS, Inc., Chicago, IL).

RESULTS

Clinical and Echocardiographic Characteristics

Nineteen patients exhibited massive APTE representing RV dysfunction and hemodynamic exacerbation, and 18 patients exhibited submassive APTE representing RV dysfunction without hemodynamic instability. The CPAH group was composed of 12 patients with idiopathic pulmonary arterial hypertension, 16 with chronic thromboem-

bolic pulmonary hypertension, seven with connective tissue disorder, and one with portopulmonary hypertension. Table 1 shows the clinical characteristics and echocardiographic hemodynamic parameters of the study groups. There were fewer men in the CPAH group compared with the other two groups. Although there were no statistical differences in systolic blood pressure among the three groups, heart rate was significantly higher in the CPAH group compared with the control group, and the elevation of heart rate in the APTE group was more pronounced than that in the CPAH group. There were no statistical differences in QRS duration among the three groups. Although the CPAH group had more pronounced high systolic pulmonary artery pressure than that in the APTE group, PVR was similar in both patient groups. There were no statistical differences in systemic vascular resistance among the three groups.

Table 2 shows the echocardiographic data of the study subjects. Although the CPAH group had larger RV chamber size compared with the APTE group, RV fractional area change was similarly reduced in both patient groups. The APTE group had smaller LV chamber size associated with lower stroke volume index compared with the other two groups. LV ejection fractions were similar in the three groups.
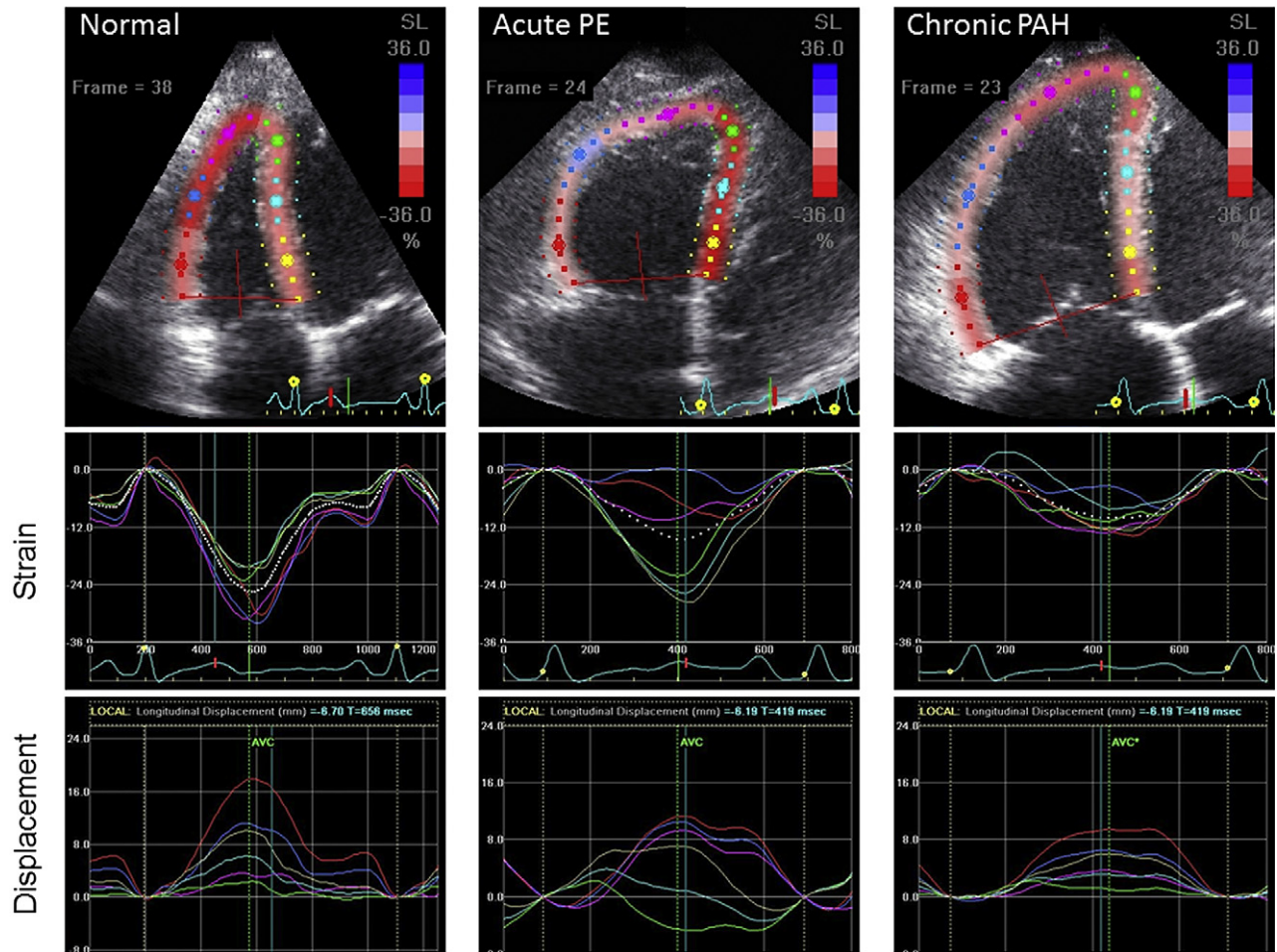
Figure 2 Examples of RV strain imaging in the RV-focused apical four-chamber view (*top*) and corresponding time-strain (*middle*) and time-displacement (*bottom*) curves from a normal subject (*left*), a patient with massive APTE (*middle*), and a patient with severe CPAH (*right*).

The LV eccentricity index was similarly high in both patient groups compared with that in the control group. Both patient groups had reduced mitral E/A ratios and Ea values compared with the control group, but mitral E/Ea ratios were higher only in the CPAH group. RV and LV MPIs were similarly high in both patient groups compared with those in the control group.

Displacement and Strain Measurements

Speckle-tracking was possible in 100% of 636 attempted segments in the RV apical four-chamber view, 98% in the LV apical four-chamber view, and 99% in the LV short-axis view, from the 106 echocardiographic studies with technically adequate images. Figures 2 and 3 show typical examples of strain imaging (*top*) and corresponding time-strain (*middle*) and time-displacement curves (*bottom*) in a normal subject, a patient with massive APTE, and a patient with severe CPAH. A normal subject had synchronous RV and LV regional strain and displacement through a cardiac cycle (Figures 2 and 3, *left*, and Video 1 for the LV longitudinal displacement image; available at www.onlinejase.com). In contrast, dyssynchronous RV and LV longitudinal regional myocardial shortening and wall motion were observed in a patient with massive APTE and a patient with severe CPAH (Figures 2 and 3, respectively,

middle and *right*). Notably, the patient with APTE had larger dispersions of longitudinal regional time-displacement curves with abnormal septal motion in the left ventricle than the patient with CPAH throughout the entire cardiac cycle (Videos 2 and 3 for LV longitudinal displacement images; available at www.onlinejase.com). Table 3 and Figure 4 show comparisons of global and segmental PSS in the 3 groups. Apical-to-lateral RV longitudinal PSS was reduced in the both patient groups, resulting in reduced global PSS compared with the control group. Notably, mid to basal lateral segments in the APTE group were distinctly reduced compared with the CPAH group. Regional LV longitudinal PSS was impaired, except for basal segments, resulting in reduced global PSS in the APTE group. In the CPAH group, although regional PSS in the mid to basal septum was reduced, global PSS was maintained, because of preserved apical-to-lateral PSS. Global and regional LV radial PSS was reduced in both patient groups to the same extent. Global and regional circumferential PSS was impaired in the APTE group. In the CPAH group, although regional PSS in the anteroseptal, anterior, and lateral segments were reduced, the other three segments were maintained, resulting in only mild reduction in global PSS. Comparisons of PSS dyssynchrony and PSD dyssynchrony in both ventricles among the three groups are shown in Table 3. All dyssynchrony indices except LV radial PSS dyssynchrony
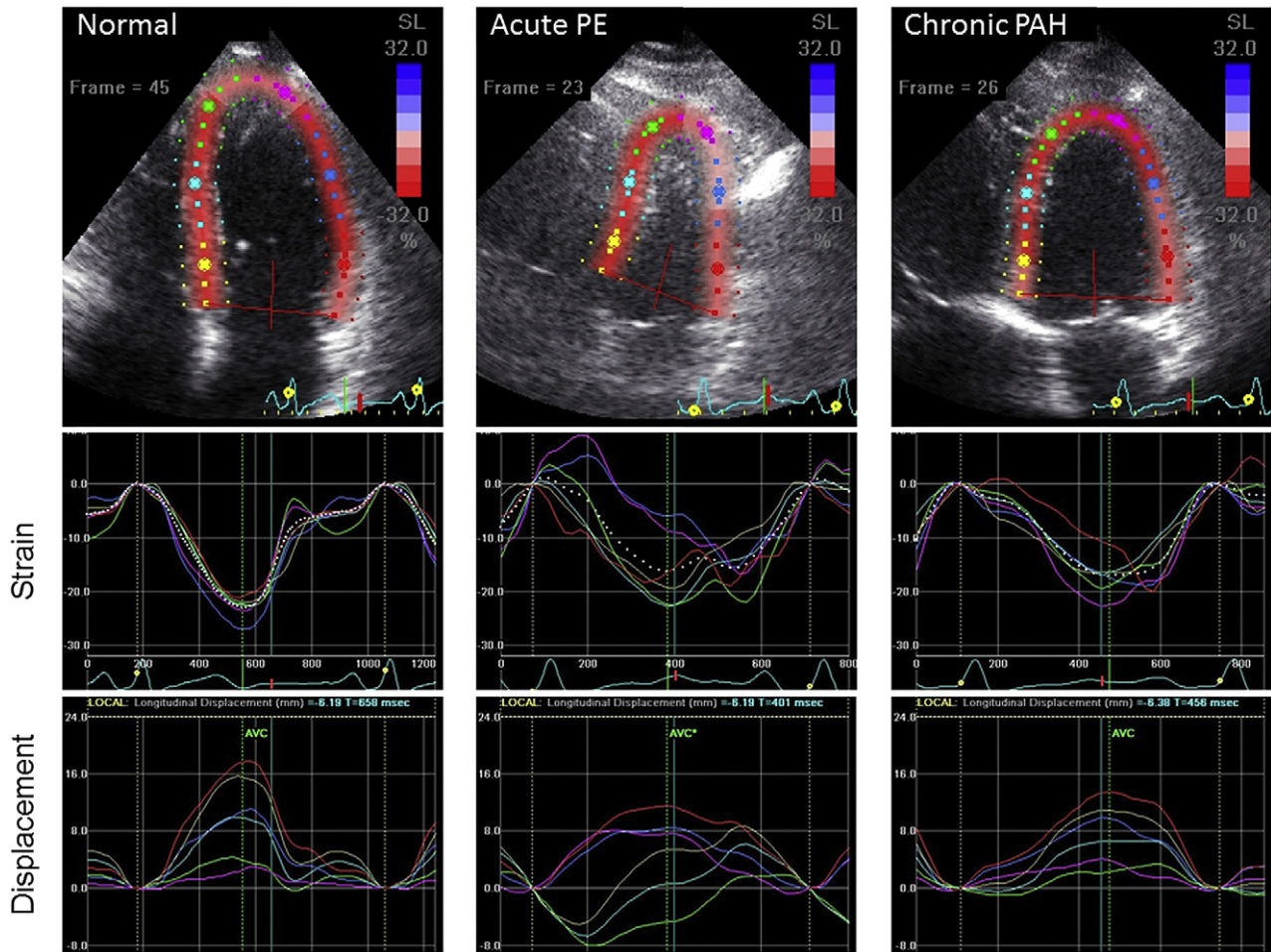
Figure 3 Examples of LV longitudinal strain imaging in the LV-focused apical four-chamber view (*top*) and corresponding time-strain (*middle*) and time-displacement (*bottom*) curves from the same normal subject (*left*), the same patient with massive APTE (*middle*), and the same patient with severe CPAH (*right*) as shown in Figure 2.

were significantly greater in both the APTE and CPAH groups compared with those in the control group. In particular, LV longitudinal PSS dyssynchrony and PSD dyssynchrony were significantly greater in the APTE group compared with those in the CPAH group.

Determinants of Ventricular Performance

There was a significant correlation between RV and LV MPI in both patient groups (Figure 5). Univariate correlation coefficients for electrocardiographic and echocardiographic variables with RV and LV MPIs and the results of the stepwise multivariate regression analyses are presented in Tables 4 and 5, respectively. PVR in the APTE group and PVR and RV end-diastolic area index in the CPAH group were independent determinants of RV MPI. In contrast, LV longitudinal PSD dyssynchrony in the APTE group and heart rate and LV eccentricity index in the CPAH group were independent determinants of LV MPI.

Interobserver and intraobserver variability were 4.2 ± 4.4% and 4.6 ± 5.5% for time to PSS and 4.5 ± 5.5% and 4.2 ± 5.3% for time to PSD in the RV longitudinal direction. In the LV longitudinal direction, they were 4.6 ± 7.7% and 4.4 ± 5.7% for time to PSS and 3.7 ± 3.1% and 3.5 ± 3.2% for time to PSD. In the LV radial direction, they were 3.9 ± 2.5% and 3.4 ± 2.9% for time to PSS and 4.5 ± 3.8% and 4.0 ± 3.6% for time to PSD. In the LV circumferen-

tial direction, they were 5.2 ± 4.6% and 4.9 ± 3.5% for time to PSS. These results indicate that intraobserver and interobserver reproducibility was acceptable.

DISCUSSION

The major findings of our study include the following: (1) both acute and chronic RV pressure overload reduced regional strain, generated mechanical dyssynchrony, and impaired myocardial performance in the right and left ventricles, (2) acute RV pressure overload is more likely to generate LV mechanical dyssynchrony and impair LV function compared with chronic RV pressure overload, and (3) pathophysiologic mechanisms that regulate ventricular performance vary depending on whether the ventricles are exposed to acute or chronic RV pressure overload.

Consistent with previous clinical observations, patients with APTE and CPAH had large RV chamber size, reduced RV systolic function, and LV chamber compression associated with abnormally high PVR.[5,6,18-20] Detailed echocardiographic assessment revealed a distinct functional impairment in the basal to mid RV lateral walls in patients with APTE, which contributed to the pathogenesis of the McConnell sign.[3] Meanwhile, patients with CPAH had very advanced RV remodeling compared with those with APTE, as

Table 1 Clinical characteristics of the study subjects

Variable	Controls (n = 33)	Patients with APTE (n = 37)	Patients with CPAH (n = 36)
Mean age (y)	57 ± 14	61 ± 15	55 ± 19
Men	45%	35%	11%*,†
Height (cm)	159 ± 10	160 ± 11	156 ± 8
Weight (kg)	56 ± 12	64 ± 19	51 ± 12†
Body mass index (kg/m²)	22 ± 3	25 ± 6*	21 ± 4†
Systolic blood pressure (mm Hg)	117 ± 12	121 ± 22	112 ± 19
Diastolic blood pressure (mm Hg)	69 ± 10	79 ± 17*	70 ± 14†
Heart rate (beats/min)	63 ± 10	93 ± 15*	76 ± 16*,†
QRS duration (msec)	87 ± 8	90 ± 12	90 ± 18
Systolic pulmonary artery pressure (mm Hg)	—	54 ± 17	77 ± 28†
PVR (Wood units)	—	5.0 ± 2.4	4.5 ± 2.0
SVR (Wood units)	20.1 ± 3.7	23.2 ± 7.6	24.1 ± 9.1

SVR, Systemic vascular resistance.
*P < .05 versus controls.
†P < .05 versus patients with APTE.

Table 2 Echocardiographic data of the study subjects

Variable	Controls (n = 33)	Patients with APTE (n = 37)	Patients with CPAH (n = 36)
RV EDA index (cm²/m²)	9 ± 2	14 ± 2*	17 ± 4*,†
RV ESA index (cm²/m²)	4 ± 1	10 ± 2*	12 ± 4*,†
RV FAC (%)	52 ± 5	28 ± 7*	29 ± 8*
LV EDV index (mL/m²)	42 ± 8	29 ± 9*	40 ± 14†
LV ESV index (mL/m²)	15 ± 4	11 ± 5*	14 ± 7
LV ejection fraction (%)	66 ± 5	63 ± 7	68 ± 9
LV eccentricity index	1.05 ± 0.06	1.47 ± 0.27*	1.51 ± 0.40*
Stroke volume index (mL/m²)	40 ± 6	25 ± 7*	30 ± 10*,†
Mitral E/A ratio	1.0 ± 0.4	0.7 ± 0.3*	0.8 ± 0.3*
Mitral Ea (cm/sec)	6.3 ± 1.9	5.4 ± 2.0*	4.5 ± 1.4*
Mitral E/Ea ratio	10 ± 3	10 ± 3	13 ± 5*,†
RV MPI	0.27 ± 0.11	0.71 ± 0.21*	0.70 ± 0.26*
LV MPI	0.40 ± 0.10	0.66 ± 0.18*	0.58 ± 0.19*

EDA, End-diastolic area; *EDV*, end-diastolic volume; *ESA*, end-systolic area; *ESV*, end-systolic volume; *FAC*, fractional area change.
*P < .05 versus controls.
†P < .05 versus patients with APTE.

Table 3 Global RV and LV PSS

Variable	Controls (n = 33)	Patients with APTE (n = 37)	Patients with CPAH (n = 36)
Global RV longitudinal PSS (%)	−26 ± 4	−14 ± 4*	−16 ± 5*
Global LV longitudinal PSS (%)	−20 ± 2	−16 ± 3*	−20 ± 4†
Global LV radial PSS (%)	55 ± 15	40 ± 16*	39 ± 14*
Global circumferential PSS (%)	−23 ± 4	−17 ± 5*	−21 ± 5*,†
RV PSS dyssynchrony (msec)	38 ± 17	94 ± 42*	83 ± 37*
RV PSD dyssynchrony (msec)	68 ± 33	106 ± 52*	107 ± 54*
LV PSS dyssynchrony (longitudinal) (msec)	43 ± 14	87 ± 33*	63 ± 22*,†
LV PSD dyssynchrony (longitudinal) (msec)	58 ± 41	119 ± 49*	83 ± 37*,†
LV PSS dyssynchrony (radial) (msec)	25 ± 23	25 ± 29	22 ± 29
LV PSD dyssynchrony (radial) (msec)	38 ± 21	71 ± 34*	65 ± 35*
LV PSS dyssynchrony (circumferential) (msec)	34 ± 21	66 ± 38*	56 ± 21*

*P < .05 versus controls.
†P < .05 versus patients with APTE.

a consequence of chronic RV pressure overload. Speckle-tracking echocardiography also demonstrated that both acute and chronic RV pressure overload induced large RV mechanical dyssynchrony to the same extent when the severity of RV pressure overload was comparable, despite a normal ventricular electrical conduction system.[4,21,22]
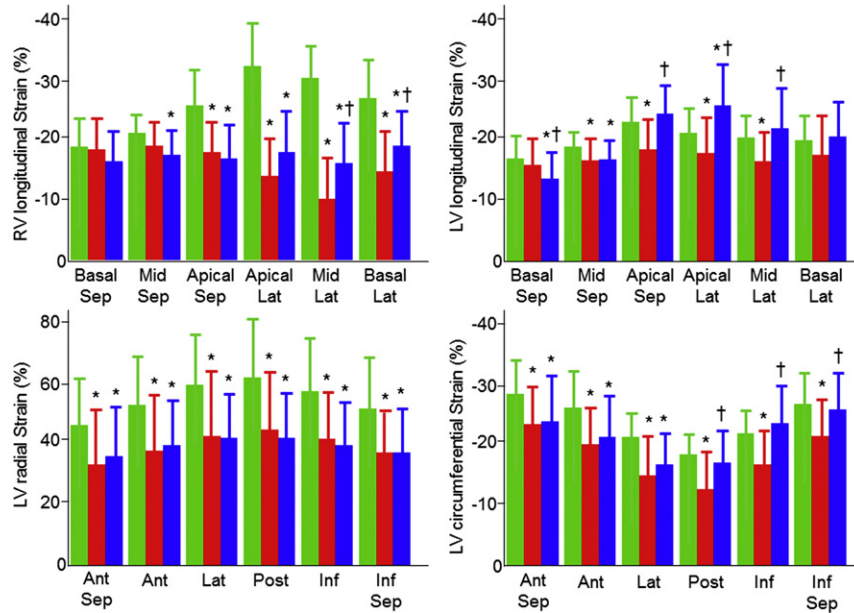
Figure 4 Bar graph showing segmental PSS in the RV longitudinal direction (*left top*), LV longitudinal direction (*right top*), LV radial direction (*right bottom*), and LV circumferential direction (*left bottom*) in normal subjects (*green bars*; n = 33), patients with APTE (*red bars*; n = 37), and patients with CPAH (*blue bars*; n = 36). Data are expressed as mean ± SD. *Ant*, Anterior wall; *Ant-Sep*, anteroseptum; *Inf*, inferior wall; *Inf-Sep*, inferoseptum; *Lat*, lateral wall; *Post*, posterior wall; *Sep*, septum. *P < .05 versus normal subjects; †P < .05 versus patients with APTE.
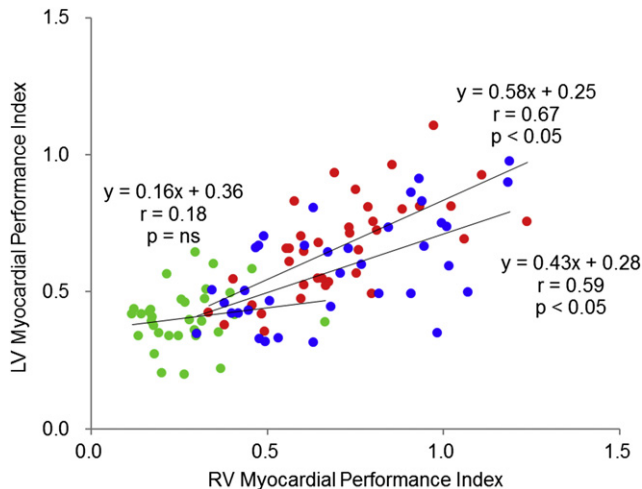

Figure 5 Relationships between RV and LV MPIs in normal subjects (*green circles*), patients with APTE (*red circles*), and patients with CPAH (*blue circles*).

An inverted transseptal pressure gradient leads to a leftward displacement and paradoxical motion of the interventricular septum in the setting of RV pressure overload,[23] resulting in impaired LV systolic and diastolic function.[24,25] MPIs in the right and left ventricles correlated in both patient groups in the present study, indicating that LV myocardial performance is regulated by ventricular interdependence.[26,27] We also elucidated that the extent and pattern of regional LV dysfunction varies depending on whether the left ventricle is exposed to acute or chronic RV pressure overload. For example, global LV longitudinal systolic strain was impaired because of reduced regional PSS in the septal, apical, and lateral segments in patients with APTE, whereas PSS maintained in the apical and lateral segments prevented global LV longitudinal

functional deterioration in patients with CPAH. It is difficult to clarify or explain the underlying mechanisms that produce these heterogeneous LV responses to acute and chronic RV pressure overload. Chronic development of RV pressure overload may cause LV free wall functional adaptation against septal dysfunction that progresses as part of RV remodeling.

We found that both acute and chronic RV pressure overload generated LV mechanical dyssynchrony. Interestingly, LV longitudinal dyssynchrony was more pronounced in the acute setting of RV pressure overload. Although simultaneous pressure recording and three-dimensional myocardial tracking in both the left and right ventricles would be warranted for the precise understanding of the pathophysiologic mechanism responsible for these complex phenomena,[28] functional maladaptation to acute RV pressure overload in the LV myocardium associated with a combination of insults, including acidosis, coronary hypotension, and hypoxemia, may induce large LV mechanical dyssynchrony associated with paradoxical septal motion.[29]

RV MPI was independently associated with PVR in patients with ATPE, whereas it was independently associated with both PVR and RV size in patients with CPAH. These results may suggest that acute and excessive RV afterload directly worsened RV performance, whereas the subsequent development of RV remodeling contributes significantly to poor RV performance. We further found that the pathophysiologic mechanisms that regulate LV performance vary depending on whether the ventricles are exposed to acute or chronic RV pressure overload. LV MPI was independently associated with LV longitudinal PSD dyssynchrony in patients with ATPE, suggesting that longitudinal LV wall motion dyssynchrony with paradoxical septal motion induced by acute RV pressure overload plays a key role in worsening LV performance. In contrast, LV MPI was independently associated with LV eccentricity index in patients with CPAH, suggesting that the geometric LV alteration secondary to chronic RV remodeling contributes significantly to poor LV performance in patients with

Table 4 Relationships between RV MPI and echocardiographic variables

	APTE			CPAH		
Variable	r	Univariate P	Multivariate P	r	Univariate P	Multivariate P
Heart rate	0.42	<.05	NS	0.22	NS	NS
QRS interval	0.01	NS	NS	0.04	NS	NS
PVR	0.59	<.05	<.05	0.50	<.05	<.05
RV EDA index	0.07	NS	NS	0.46	<.05	<.05
RV PSS dyssynchrony	0.17	NS	NS	0.42	<.05	NS
RV PSD dyssynchrony	0.04	NS	NS	0.20	NS	NS

EDA, End-diastolic area.

Table 5 Relationships between LV MPI and echocardiographic variables

	APTE			CPAH		
Variable	r	Univariate P	Multivariate P	r	Univariate P	Multivariate P
Heart rate	0.33	<.05	NS	0.51	<.05	<.05
QRS interval	−0.15	NS	NS	−0.20	NS	NS
SVR	0.25	NS	NS	−0.03	NS	NS
LV EDV index	−0.21	NS	NS	−0.38	<.05	NS
EI	0.18	NS	NS	0.54	<.05	<.05
LV PSS dyssynchrony (longitudinal)	0.37	<.05	NS	0.02	NS	NS
LV PSD dyssynchrony (longitudinal)	0.66	<.05	<.05	0.41	<.05	NS
LV PSS dyssynchrony (radial)	−0.07	NS	NS	0.14	NS	NS
LV PSD dyssynchrony (radial)	0.25	NS	NS	0.18	NS	NS
LV PSS dyssynchrony (circumferential)	0.37	<.05	NS	−0.12	NS	NS

EI, Eccentricity index; *EDV*, end-diastolic volume; *SVR*, systemic vascular resistance.

chronic RV pressure overload (Figure 6). A number of studies have shown that RV pressure overload affects LV function not only by limiting LV preload but also by abnormal pressure interaction via the intraventricular septum and the pericardium, known as ventricular interdependence.[23-27] However, this is the first study to investigate the potential role of regional wall motion abnormalities and mechanical dyssynchrony in the pathophysiologic processes leading to the development of LV functional deterioration using speckle-tracking echocardiography in combination with quantitative assessment of ventricular geometric remodeling in both acute and chronic RV pressure overload. Because impaired longitudinal function has been known to be not only a sensitive marker for identifying early myocardial damage but also a reliable predictor of a negative prognosis in patients with various heart diseases, noninvasive assessment of segmental wall motion and synchrony, especially in the longitudinal direction, can provide useful insight into the pathophysiology of ventricular interdependence in patients with RV pressure overload.

Study Limitations

Invasive pressure measurements were not used in this study. Therefore, peak systolic RV pressure and PVR estimated using Doppler echocardiography were recruited as markers of the severity of RV pressure overload. However, Doppler-derived estimations of these hemodynamic indices are well recognized to correlate well with simultaneous catheter-derived measurements and are widely used clinically.

We assessed longitudinal LV kinetics only in the apical four-chamber view, mainly because the apical two-chamber and long-axis views were suboptimal for speckle-tracking analysis mainly because of severe LV deformation in certain patients. Indeed, LV longitudinal function and synchrony in patients with RV dysfunction have been assessed only in the apical four-chamber view in most clinical studies.[5,30,31] Therefore, although still far from conclusive, our approach might provide a clinically adequate model to evaluate LV function and synchrony.

We did not perform circumferential displacement analysis in the present study, because EchoPAC has no capability to measure circumferential displacement. During LV systole, the base rotates in an overall clockwise direction and the apex rotates in a counterclockwise direction when viewed from apex to base, resulting in LV torsion. However, the rotation (i.e., circumferential myocardial displacement) is minimal and hardly contributes to ventricular ejection at the mid-ventricular level.

It has been recognized that LV performance is impaired by decreased LV distensibility caused by a leftward shift of the interventricular septum and of pericardial restraint caused by right heart failure, both of which are related to the degree RV dilatation.[32] However, it was not possible to quantify LV distensibility using invasive LV pressure-volume loop analysis in the present study.

Finally, evaluation of the clinical outcome was not included in our study. The long-term effects of LV regional nonuniformity on morbidity and mortality warrant further investigation.

CONCLUSIONS

Speckle-tracking echocardiography effectively quantified ventricular function and dyssynchrony both in the right and left ventricles in
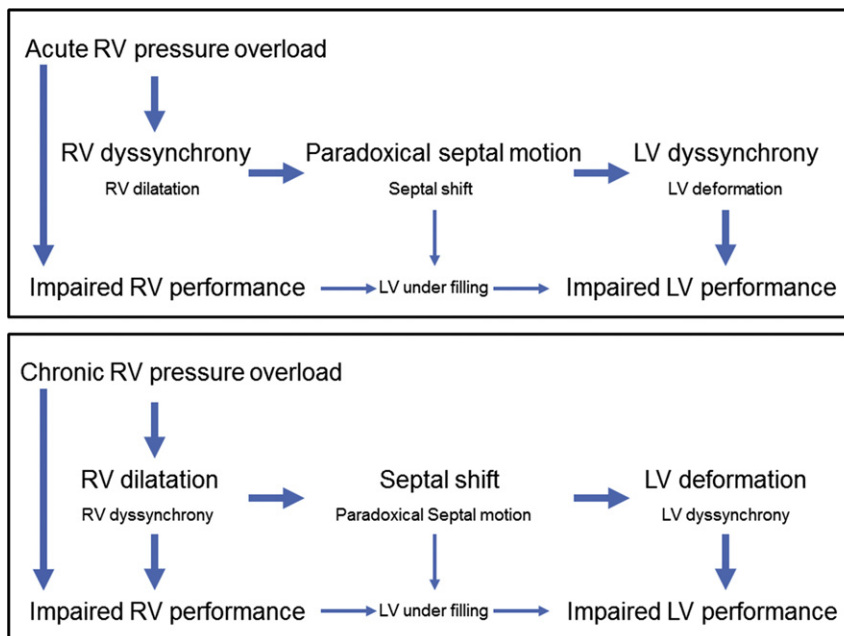
Figure 6 Flowcharts of the proposed pathophysiologic mechanisms that regulate ventricular performance in acute and chronic RV pressure overload.

patients with APTE and CPAH. The pathophysiologic mechanisms that regulate ventricular performance vary depending on whether the ventricles are exposed to acute or chronic RV pressure overload. Application of speckle-tracking echocardiography to conventional measurements of ventricular function could provide a more thorough and quantitative pathophysiologic characterization of functional RV and LV adaptation to acute and chronic RV pressure overload and contribute to a better understanding how RV pressure overload worsens ventricular performance.

REFERENCES

1. Haddad F, Doyle R, Murphy DJ, Hunt SA. Right ventricular function in cardiovascular disease, part II: pathophysiology, clinical importance, and management of right ventricular failure. Circulation 2008;117:1717-31.
2. Kasner M, Westermann D, Steendijk P, Drose S, Poller W, Schultheiss HP, et al. LV dysfunction induced by a non-severe idiopathic pulmonary arterial hypertension. A pressure-volume relationship study. Am J Respir Crit Care Med 2012;186:181-9.
3. Sugiura E, Dohi K, Onishi K, Takamura T, Tsuji A, Ota S, et al. Reversible right ventricular regional non-uniformity quantified by speckle-tracking strain imaging in patients with acute pulmonary thromboembolism. J Am Soc Echocardiogr 2009;22:1353-9.
4. Kalogeropoulos AP, Georgiopoulou VV, Howell S, Pernetz MA, Fisher MR, Lerakis S, et al. Evaluation of right intraventricular dyssyn-

chrony by two-dimensional strain echocardiography in patients with pulmonary arterial hypertension. J Am Soc Echocardiogr 2008;21:1028-34.
5. Takamura T, Dohi K, Onishi K, Sakurai Y, Ichikawa K, Tsuji A, et al. Reversible left ventricular regional non-uniformity quantified by speckle-tracking displacement and strain imaging in patients with acute pulmonary embolism. J Am Soc Echocardiogr 2011;24:792-802.
6. Dohi K, Onishi K, Gorcsan J III, Lopez-Candales A, Takamura T, Ota S, et al. Role of radial strain and displacement imaging to quantify wall motion dyssynchrony in patients with left ventricular mechanical dyssynchrony and chronic right ventricular pressure overload. J Am Coll Cardiol 2008;101:1206-12.
7. Suffoletto MS, Dohi K, Cannesson M, Saba S, Gorcsan J III. Novel speckle-tracking radial strain from routine black-and-white echocardiographic images to quantify dyssynchrony and predict response to cardiac resynchronization therapy. Circulation 2006;113:960-8.
8. Galie N, Hoeper MM, Humbert M, Torbicki A, Vachiery JL, Barbera JA, et al. Guidelines for the diagnosis and treatment of pulmonary hypertension. Eur Respir J 2009;34:1219-63.
9. Torbicki A, Perrier A, Konstantinides S, Agnelli G, Galie N, Pruszczyk P, et al. Guidelines on the diagnosis and management of acute pulmonary embolism: the Task Force for the Diagnosis and Management of Acute Pulmonary Embolism of the European Society of Cardiology. Eur Heart J 2008;29:2276-315.
10. Eid-Lidt G, Gaspar J, Sandoval J, de los Santos FD, Pulido T, Gonzalez Pacheco H, et al. Combined clot fragmentation and aspiration in patients with acute pulmonary embolism. Chest 2008;134:54-60.
11. Rudski LG, Lai WW, Afilalo J, Hua L, Handschumacher MD, Chandrasekaran K, et al. Guidelines for the echocardiographic assessment of the right heart in adults: a report from the American Society of Echocardiography endorsed by the European Association of Echocardiography, a registered branch of the European Society of Cardiology, and the Canadian Society of Echocardiography. J Am Soc Echocardiogr 2010;23:685-713.
12. Abbas AE, Fortuin FD, Schiller NB, Appleton CP, Moreno CA, Lester SJ. A simple method for noninvasive estimation of pulmonary vascular resistance. J Am Coll Cardiol 2003;41:1021-7.
13. Katz WE, Gasior TA, Quinlan JJ, Lazar JM, Firestone L, Griffith BP, et al. Immediate effects of lung transplantation on right ventricular morphology

and function in patients with variable degrees of pulmonary hypertension. J Am Coll Cardiol 1996;27:384-91.

14. Takamura T, Dohi K, Onishi K, Tanabe M, Sugiura E, Nakajima H, et al. Left ventricular contraction-relaxation coupling in normal, hypertrophic, and failing myocardium quantified by speckle-tracking global strain and strain rate imaging. J Am Soc Echocardiogr 2010;23:747-54.

15. Nagueh SF, Middleton KJ, Kopelen HA, Zoghbi WA, Quinones MA. Doppler tissue imaging: a noninvasive technique for evaluation of left ventricular relaxation and estimation of filling pressures. J Am Coll Cardiol 1997;30:1527-33.

16. Tei C, Ling LH, Hodge DO, Bailey KR, Oh JK, Rodeheffer RJ, et al. New index of combined systolic and diastolic myocardial performance: a simple and reproducible measure of cardiac function—a study in normals and dilated cardiomyopathy. J Cardiol 1995;26:357-66.

17. Tei C, Dujardin KS, Hodge DO, Bailey KR, McGoon MD, Tajik AJ, et al. Doppler echocardiographic index for assessment of global right ventricular function. J Am Soc Echocardiogr 1996;9:838-47.

18. Mori S, Nakatani S, Kanzaki H, Yamagata K, Take Y, Matsuura Y, et al. Patterns of the interventricular septal motion can predict conditions of patients with pulmonary hypertension. J Am Soc Echocardiogr 2008;21:386-93.

19. Goldhaber SZ. Echocardiography in the management of pulmonary embolism. Ann Intern Med 2002;136:691-700.

20. Fukuda Y, Tanaka H, Sugiyama D, Ryo K, Onishi T, Fukuya H, et al. Utility of right ventricular free wall speckle-tracking strain for evaluation of right ventricular performance in patients with pulmonary hypertension. J Am Soc Echocardiogr 2011;24:1101-8.

21. Lopez-Candales A, Dohi K, Bazaz R, Edelman K. Relation of right ventricular free wall mechanical delay to right ventricular dysfunction as determined by tissue Doppler imaging. Am J Cardiol 2005;96:602-6.

22. Marcus JT, Gan CT, Zwanenburg JJ, Boonstra A, Allaart CP, Gotte MJ, et al. Interventricular mechanical asynchrony in pulmonary arterial hypertension: left-to-right delay in peak shortening is related to right ventricular overload and left ventricular underfilling. J Am Coll Cardiol 2008;51:750-7.

23. Jessup M, Sutton MS, Weber KT, Janicki JS. The effect of chronic pulmonary hypertension on left ventricular size, function, and interventricular septal motion. Am Heart J 1987;113:1114-22.

24. Dittrich HC, Chow LC, Nicod PH. Early improvement in left ventricular diastolic function after relief of chronic right ventricular pressure overload. Circulation 1989;80:823-30.

25. Menzel T, Wagner S, Kramm T, Mohr-Kahaly S, Mayer E, Braeuninger S, et al. Pathophysiology of impaired right and left ventricular function in chronic embolic pulmonary hypertension: changes after pulmonary thromboendarterectomy. Chest 2000;118:897-903.

26. Bove AA, Santamore WP. Ventricular interdependence. Prog Cardiovasc Dis 1981;23:365-88.

27. Chang SM, Lin CC, Hsiao SH, Lee CY, Yang SH, Lin SK, et al. Pulmonary hypertension and left heart function: insights from tissue Doppler imaging and myocardial performance index. Echocardiogr 2007;24:366-73.

28. Tanaka H, Matsumoto K, Hiraishi M, Miyoshi T, Kaneko A, Tsuji T, et al. Multidirectional left ventricular performance detected with three-dimensional speckle-tracking strain in patients with chronic right ventricular pacing and preserved ejection fraction. Eur Heart J Cardiovasc Imaging 2012;13:849-56.

29. Sullivan DM, Watts JA, Kline JA. Biventricular cardiac dysfunction after acute massive pulmonary embolism in the rat. J Appl Physiol 2001;90:1648-56.

30. Hardziyenka M, Campian ME, Verkerk AO, Surie S, van Ginneken AC, Hakim S, et al. Electrophysiologic remodeling of the left ventricle in pressure overload-induced right ventricular failure. J Am Coll Cardiol 2012;59:2193-202.

31. Howard LS, Grapsa J, Dawson D, Bellamy M, Chambers JB, Masani ND, et al. Echocardiographic assessment of pulmonary hypertension: standard operating procedure. Eur Respir Rev 2012;21:239-48.

32. Shirakabe M, Yamaguchi S, Tamada Y, Baniya G, Fukui A, Miyawaki H, et al. Impaired distensibility of the left ventricle after stiffening of the right ventricle. J Appl Physiol 2001;91:435-40.